Immunity, Volume *53*

Supplemental Information

Affinity-Restricted Memory B Cells Dominate Recall Responses to Heterologous Flaviviruses

Rachel Wong, Julia A. Belk, Jennifer Govero, Jennifer L. Uhrlaub, Dakota Reinartz, Haiyan Zhao, John M. Errico, Lucas D'Souza, Tyler J. Ripperger, Janko Nikolich-Zugich, Mark J. Shlomchik, Ansuman T. Satpathy, Daved H. Fremont, Michael S. Diamond, and Deepta Bhattacharya

Figure S1

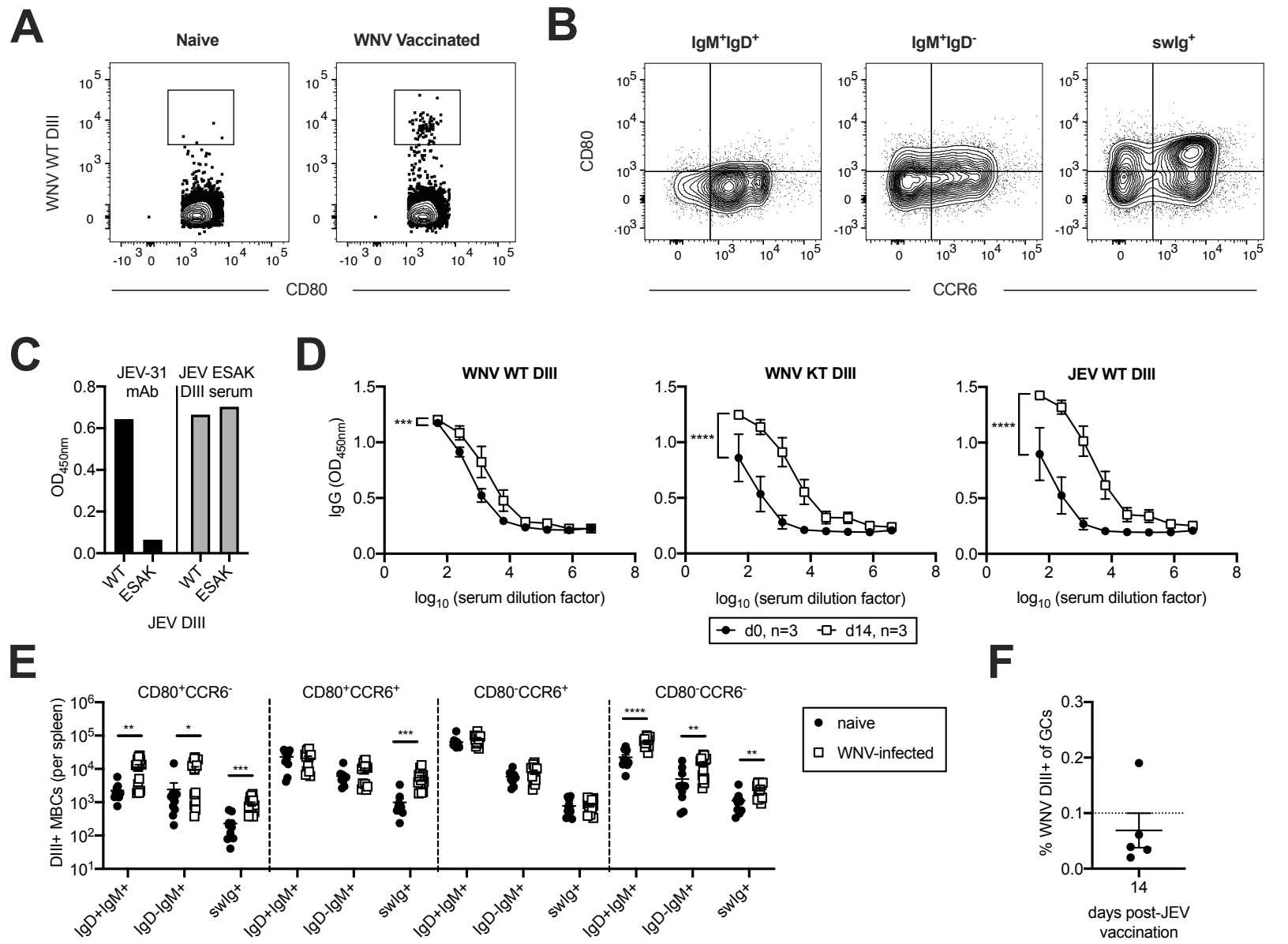
A
Naive
WNV Vaccinated
WNV WT DIII
CD80
B
IgM+IgD+
IgM+IgD-
swIg+
CD80
CCR6
C
JEV-31 mAb
JEV ESAK DIII serum
OD450nm
WT
ESAK
WT
ESAK
JEV DIII
D
WNV WT DIII
WNV KT DIII
JEV WT DIII
IgG (OD450nm)
log10 (serum dilution factor)
d0, n=3
d14, n=3
E
CD80+CCR6-
CD80+CCR6+
CD80-CCR6+
CD80-CCR6-
DIII+ MBCs (per spleen)
IgD+IgM+
IgD-IgM+
swIg+
naive
WNV-infected
F
% WNV DIII+ of GCs
14
days post-JEV vaccination

Figure S1, related to Figure 1. Memory B cell subsets and their response after heterologous challenge.

(**A**) Validation of WNV WT DIII tetramers by analyzing the swIg (IgM^-IgD^-) MBC compartment after WNV vaccination. (**B**) Gating strategy for MBC subsets based on CD80 and CCR6 expression. Cells are gated on $CD19^+GL7^-$ and IgM^+IgD^+, IgM^+IgD^-, or swIg expression. Concatenated data from one experiment is shown. (**C**) Validation of JEV ESAK DIII by ELISA. JEV DIII-LR specific mAb JEV-31 (Fernandez et al., 2018) was used to confirm loss of the LR epitope. Wild-type mice were immunized with JEV ESAK DIII, and immune serum was used to probe for binding to JEV WT and ESAK DIII. Data from 1 experiment is shown. Mean values ± SEM are shown. (**D**) Serum from WNV-immune mice before (d0) and 14 days after JEV vaccination was assessed for antibody binding to WNV WT DIII, WNV KT DIII, and JEV WT DIII. Data pooled from one experiment with 3 mice, and correspond with Figure 1D. **** , $p < 0.0001$ by 2-way ANOVA. (**E**) Enrichment of WNV DIII-specificity in different MBC subsets >8 weeks after WNV infection. (**F**) Frequency of WNV DIII-specific GC B cells 2 weeks after JEV vaccination of WNV infected mice.

Figure S2

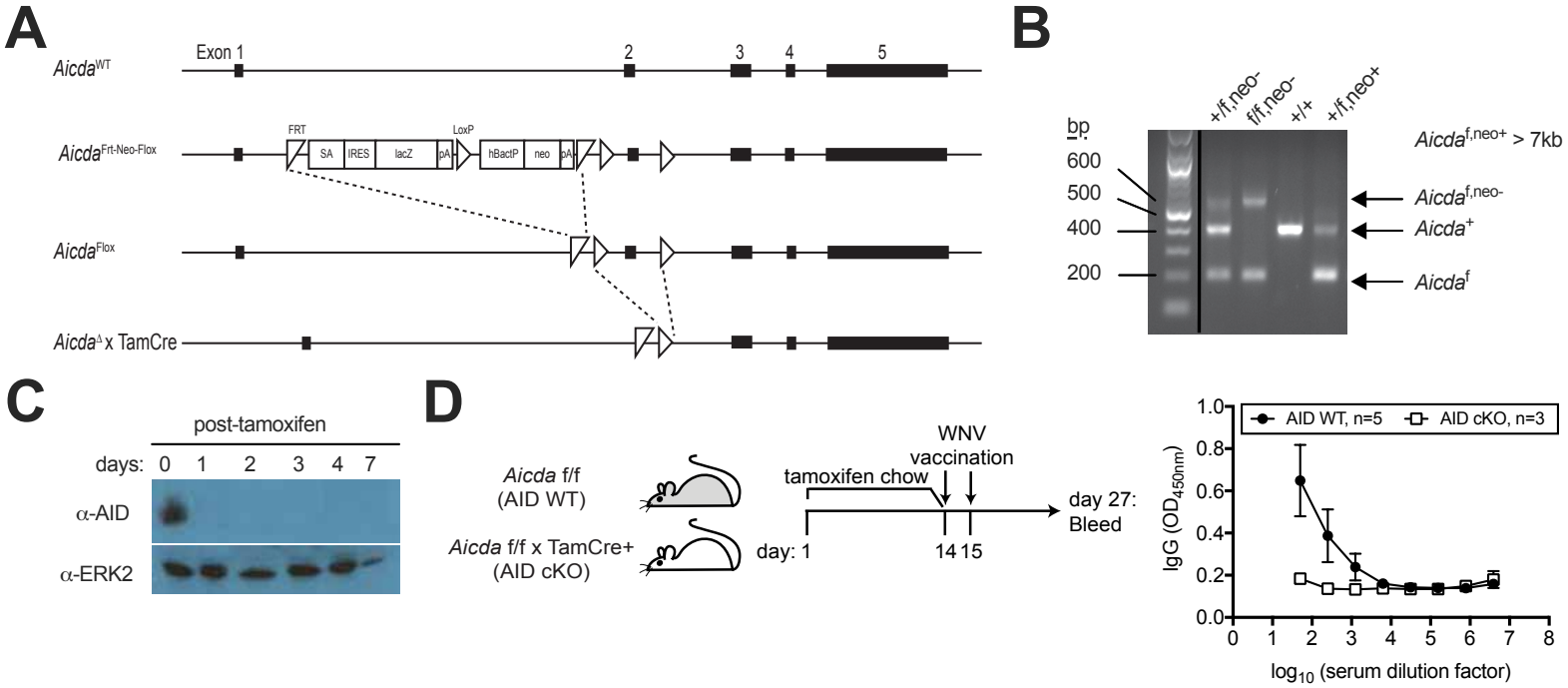
A
Aicda^WT
Exon 1
2
3
4
5
Aicda^Frt-Neo-Flox
FRT
SA
IRES
lacZ
pA
LoxP
hBactP
neo
pA
Aicda^Flox
Aicda^Δ x TamCre
B
bp
600
500
400
200
+/f,neo-
f/f,neo-
+/+
+/f,neo+
Aicda^f,neo+ > 7kb
Aicda^f,neo-
Aicda^+
Aicda^f
C
post-tamoxifen
days: 0 1 2 3 4 7
α-AID
α-ERK2
D
Aicda f/f
(AID WT)
Aicda f/f x TamCre+
(AID cKO)
tamoxifen chow
WNV
vaccination
day: 1
14 15
day 27:
Bleed
AID WT, n=5
AID cKO, n=3
IgG (OD450nm)
log10 (serum dilution factor)

Figure S2, related to Figure 2. Validation of *Aicda f/f* mice.

(**A**) Targeting construct for *Aicda*. (**B**) PCR genotyping of the *Aicda* allele to confirm targeting and absence of neomycin resistance cassette. (**C**) *Aicda*$^{f/f}$ x TamCre mice were immunized with sheep red blood cells and treated with tamoxifen starting on day 7 after immunization. CD19^{+}GL7^{+} cells were sorted at different days after tamoxifen and immunoblotted for AID. ERK2 level (probed with anti-ERK2 antibody) was used as the loading control. (**D**) *Aicda*$^{f/f}$ x TamCre mice were treated with tamoxifen for two weeks and then immunized with the inactivated WNV vaccine. Serum was collected 12 days later to confirm absence of anti-WNV WT DIII IgG antibodies. Mean values ± SEM are shown.

Figure S3

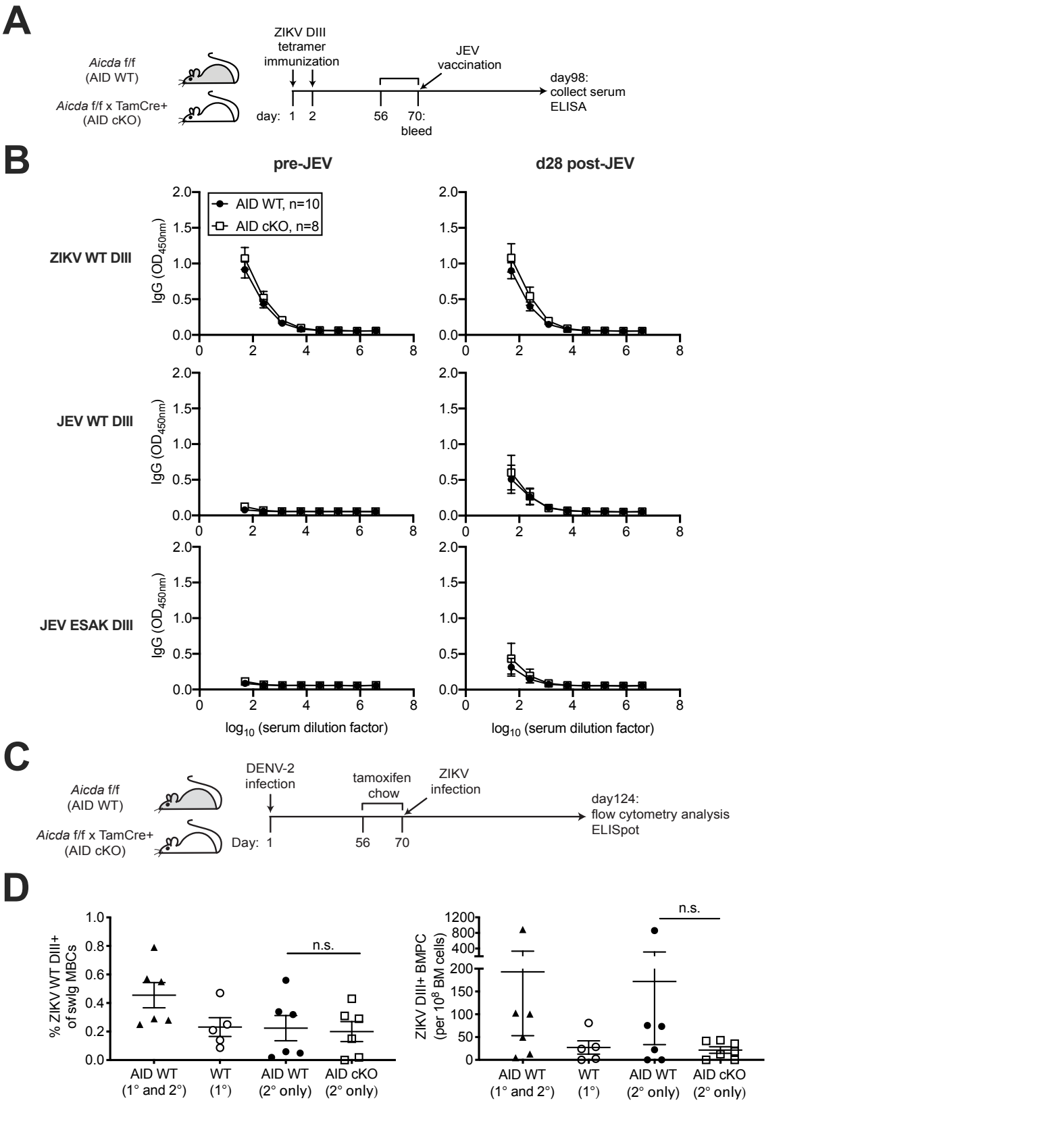
A
Aicda f/f
(AID WT)
Aicda f/f x TamCre+
(AID cKO)
ZIKV DIII
tetramer
immunization
JEV
vaccination
day: 1 2 56 70:
bleed
day98:
collect serum
ELISA
B
pre-JEV
d28 post-JEV
AID WT, n=10
AID cKO, n=8
ZIKV WT DIII
JEV WT DIII
JEV ESAK DIII
IgG (OD450nm)
log10 (serum dilution factor)
C
Aicda f/f
(AID WT)
Aicda f/f x TamCre+
(AID cKO)
DENV-2
infection
tamoxifen
chow
ZIKV
infection
Day: 1 56 70
day124:
flow cytometry analysis
ELISpot
D
% ZIKV WT DIII+
of swIg MBCs
n.s.
AID WT
(1° and 2°)
WT
(1°)
AID WT
(2° only)
AID cKO
(2° only)
ZIKV DIII+ BMPC
(per 10^8 BM cells)
n.s.
AID WT
(1° and 2°)
WT
(1°)
AID WT
(2° only)
AID cKO
(2° only)

Figure S3, related to Figure 2. IgM responses after heterologous JEV vaccination. (**A**) Schematic representation of the experimental setup for ZIKV DIII immunization and subsequent JEV recall responses. (**B**) Serum from ZIKV DIII-immunized AID cKO and AID WT was collected before and 28 days after JEV vaccination. IgG serum antibody binding to ZIKV WT DIII, JEV WT DIII, and JEV ESAK DIII at different serum dilutions was assessed by ELISA. Data are pooled from two independent experiment with 5-6 mice per genotype for each experiment. Mean values ± SEM are shown. **(C)** Schematic representation of DENV and ZIKV recall responses. (**D**) The frequency of ZIKV DIII-specific MBCs and LLPCs were quantified by flow cytometry and ELISPOT, respectively. Mice challenged with only ZIKV (1°) were used to delineate the naïve B cell responses. AID WT (2° only) is calculated by subtracting the average WT primary response value (1°) from the AID WT (1° and 2°) values. Mean values ± SEM are shown; each symbol represents one mouse. Data are pooled from two independent experiments.

Figure S4

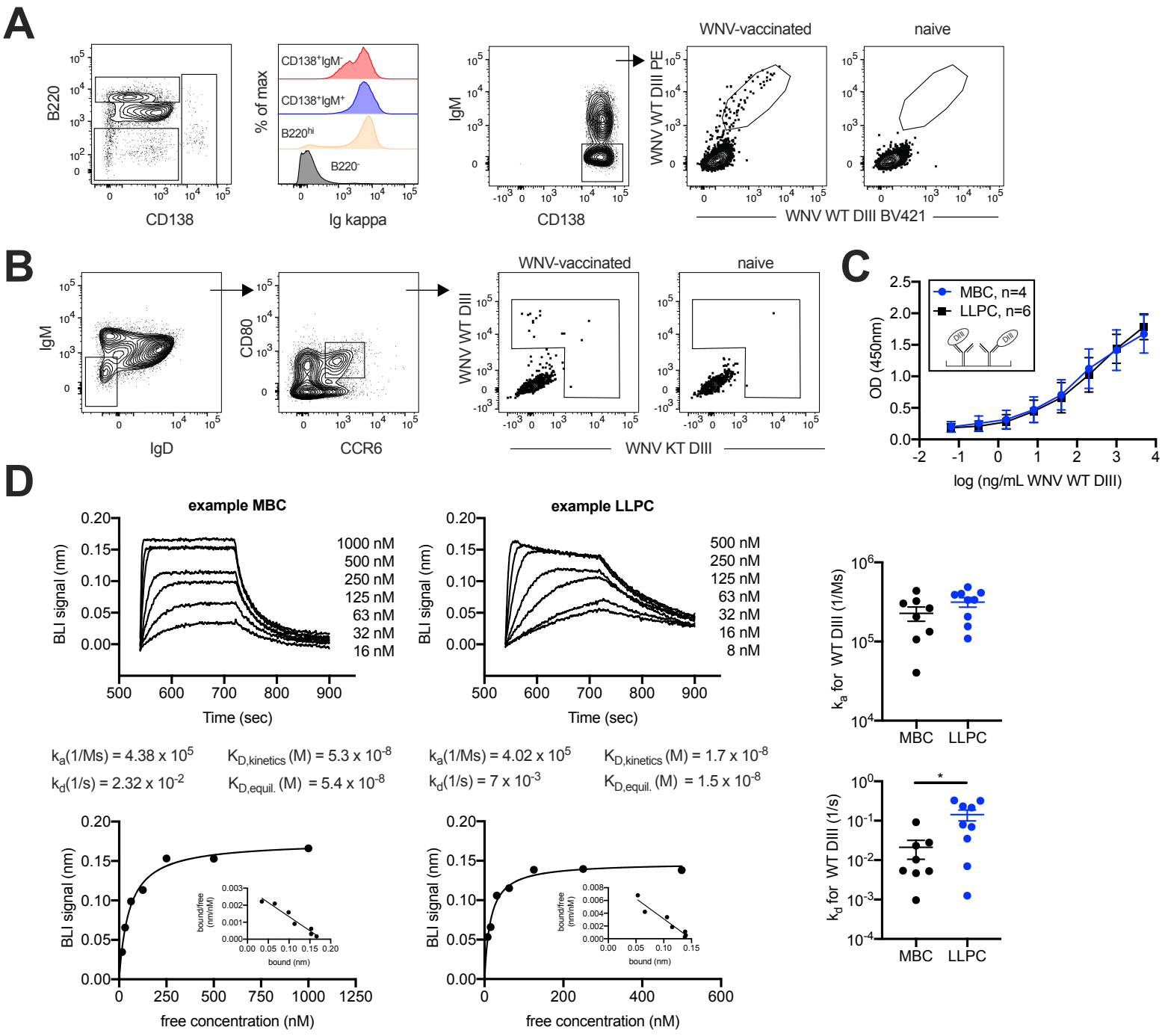
A
B220
CD138
% of max
CD138+IgM-
CD138+IgM+
B220hi
B220-
Ig kappa
IgM
CD138
WNV-vaccinated
naive
WNV WT DIII PE
WNV WT DIII BV421
B
IgM
IgD
CD80
CCR6
WNV-vaccinated
naive
WNV WT DIII
WNV KT DIII
C
MBC, n=4
LLPC, n=6
OD (450nm)
log (ng/mL WNV WT DIII)
D
example MBC
example LLPC
BLI signal (nm)
Time (sec)
1000 nM
500 nM
250 nM
125 nM
63 nM
32 nM
16 nM
8 nM
ka(1/Ms) = 4.38 x 10^5
KD,kinetics (M) = 5.3 x 10^-8
kd(1/s) = 2.32 x 10^-2
KD,equil. (M) = 5.4 x 10^-8
ka(1/Ms) = 4.02 x 10^5
KD,kinetics (M) = 1.7 x 10^-8
kd(1/s) = 7 x 10^-3
KD,equil. (M) = 1.5 x 10^-8
bound/free (nm/nM)
bound (nm)
free concentration (nM)
ka for WT DIII (1/Ms)
kd for WT DIII (1/s)
MBC
LLPC
*

Figure S4, related to Figure 4. Isolation of mAbs from MBCs and LLPCs.

(**A**) Gating strategy for WNV DIII-specific LLPCs. LLPCs were first assessed for surface B cell receptor expression by analyzing surface kappa expression. LLPCs in the bone marrow were enriched for CD138 expression followed by WNV WT DIII staining with two different tetramers. (**B**) Wild-type mice were immunized with inactivated WNV vaccine, and DIII-specific MBCs and LLPCs were sorted at least 8 weeks after vaccination. Gating strategy for $CD19^{+}GL7^{-}$ WNV DIII-specific MBCs. Splenocytes were depleted of CD3, CD4, CD8, CD11b, Ter119, IgM and IgG prior to sorting. (**C**) Reverse orientation ELISA of a subset of DIII-specific mAbs to measure monovalent affinities. ELISA plates were coated with a fixed concentration of mAbs and incubated with increasing concentrations of WNV WT DIII. Mean values ± SEM are shown. (**D**) Example binding curve (left) generated by biolayer interferometry with increasing concentrations of WNV WT DIII. Binding curves were fit to a 1:1 binding model using ForteBio's analysis software. The panel to the right of the binding curve shows steady-state analysis results ($K_{D,\ equilibrium}$), plotted as the binding response (nm) versus concentration of DIII, shows binding saturation. A Scatchard plot, shown in the inset in the steady-state analysis panel, suggests single binding affinity. The binding association (middle right) and dissociation (right) constants were calculated. Mean ± SEM are shown; each symbol represents one mAb.

Figure S5

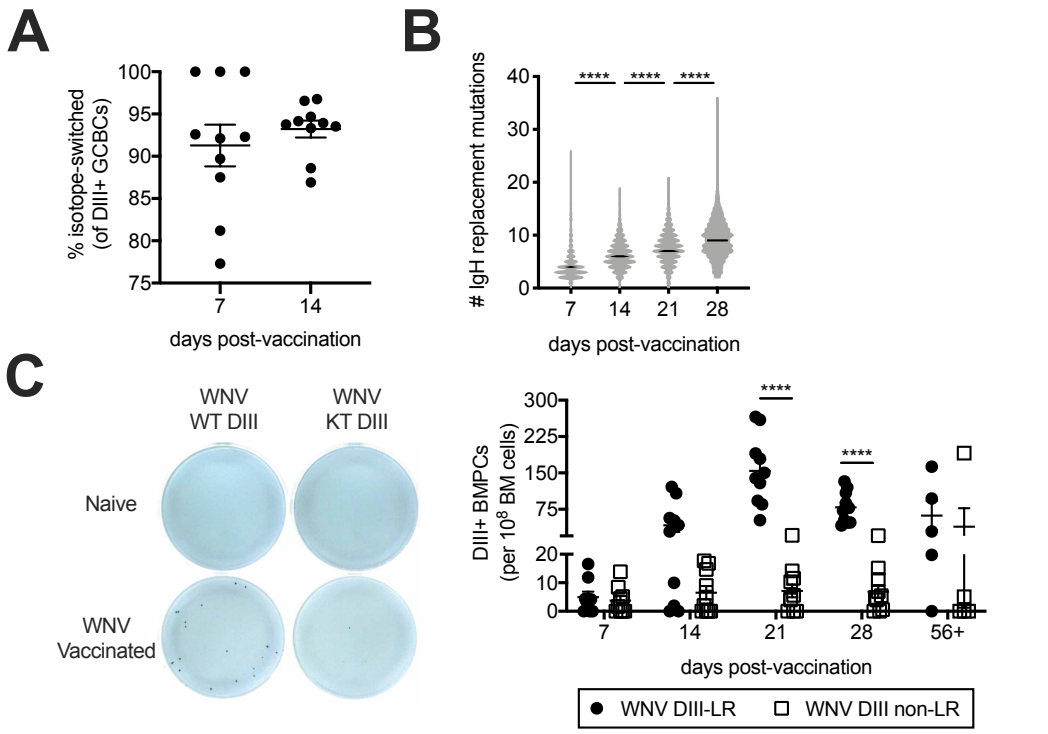
A
% isotope-switched (of DIII+ GCBCs)
days post-vaccination
B
IgH replacement mutations
****
days post-vaccination
C
WNV WT DIII
WNV KT DIII
Naive
WNV Vaccinated
DIII+ BMPCs (per 10^8 BM cells)
days post-vaccination
WNV DIII-LR
WNV DIII non-LR

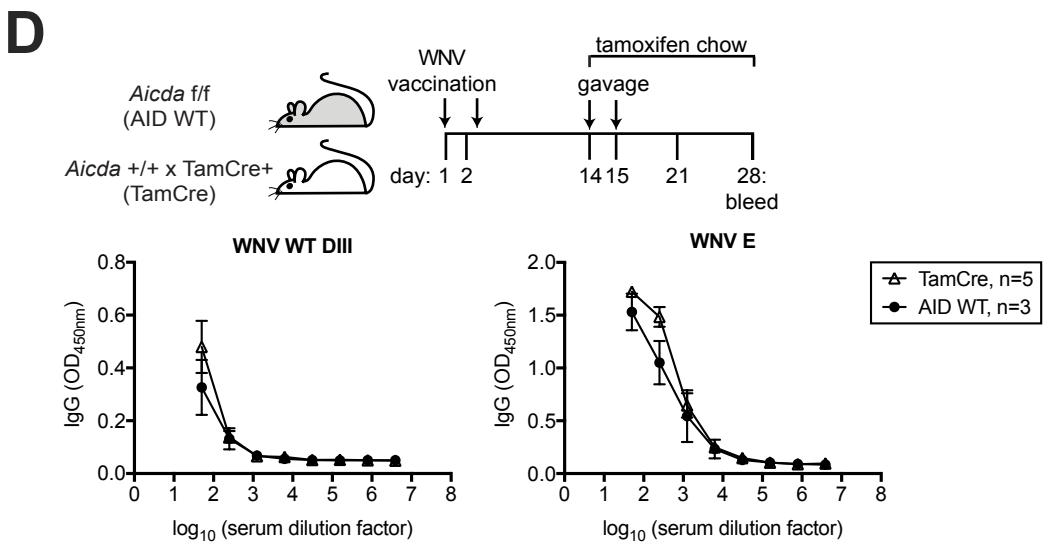
D
Aicda f/f (AID WT)
Aicda +/+ x TamCre+ (TamCre)
WNV vaccination
tamoxifen chow
gavage
day: 1 2 14 15 21 28: bleed
WNV WT DIII
WNV E
IgG (OD450nm)
log10 (serum dilution factor)
TamCre, n=5
AID WT, n=3

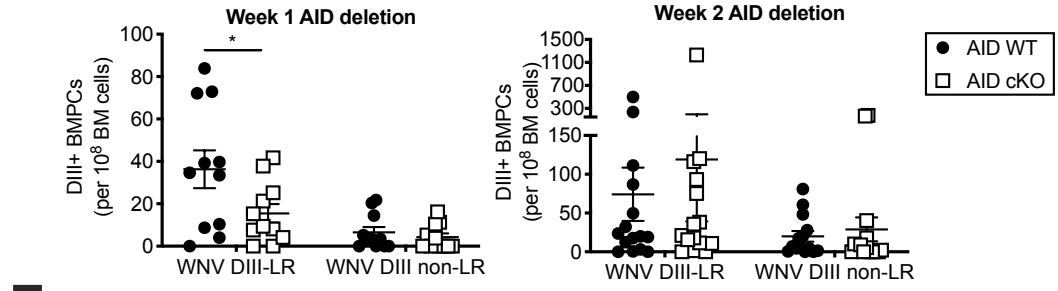
E
Week 1 AID deletion
Week 2 AID deletion
DIII+ BMPCs (per 10^8 BM cells)
AID WT
AID cKO
WNV DIII-LR
WNV DIII non-LR

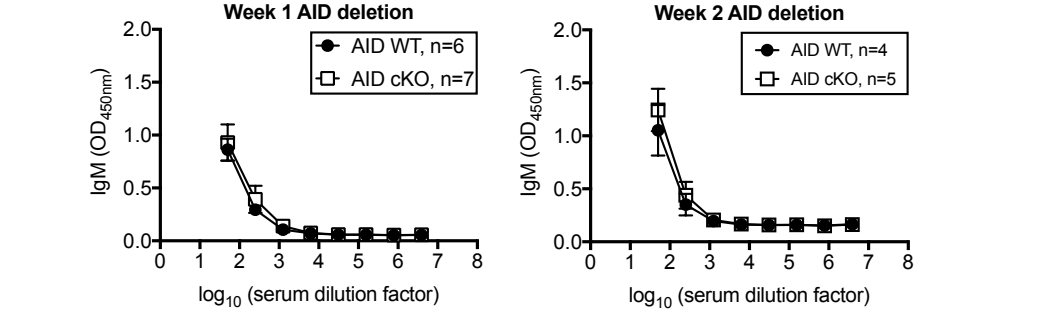
F
Week 1 AID deletion
Week 2 AID deletion
IgM (OD450nm)
log10 (serum dilution factor)
AID WT, n=6
AID cKO, n=7
AID WT, n=4
AID cKO, n=5

Figure S5, related to Figure 5. Deletion of AID during GC reactions does not impair class switching or differentiation of MBCs and LLPCs.

(**A**) Frequencies of isotype switched (IgM^-IgD^-), WNV $DIII^+$ GC B cells ($CD19^+GL7^+$) 7 and 14 days after immunization of wild-type mice with inactivated WNV vaccine as measured by flow cytometry. Mean values ± SEM are shown. Each symbol represents one mouse. Data are pooled from two independent experiments. (**B**) WT mice were immunized with inactivated WNV vaccine. WNV $DIII^+$ GC B cells ($CD19^+GL7^+IgD^-$) were sorted at different time points and IgH repertoire analysis was performed by MiSeq. The total number of replacement mutations for IgH is shown for each week. (**C**) WT mice were immunized with inactivated WNV vaccine, and the number of DIII-specific bone marrow plasma cells were enumerated by ELISPOT at different time points. Representative wells are shown on the left and quantified on the right. Mean values ± SEM are shown. Each symbol represents one mouse. Data are pooled from two independent experiments. (**D**) Schematic of experiments to test for Cre toxicity. Sera were collected 28 days after vaccination and probed for anti-WNV WT DIII and E protein IgG antibodies. Mean values ± SEM are shown. (**E**) WNV DIII-specific LLPC numbers after WNV vaccination and AID deletion were enumerated by ELISPOT. Mean values ± SEM are shown. Each symbol represents one mouse. Data are pooled from two independent experiments. (**F**) Serum from mice after WNV vaccination and AID deletion was collected 8 weeks post-immunization, and IgM antibodies were probed for WNV E reactivity by ELISA. Mean values ± SEM are shown. Data are pooled from two independent experiments.

Figure S6

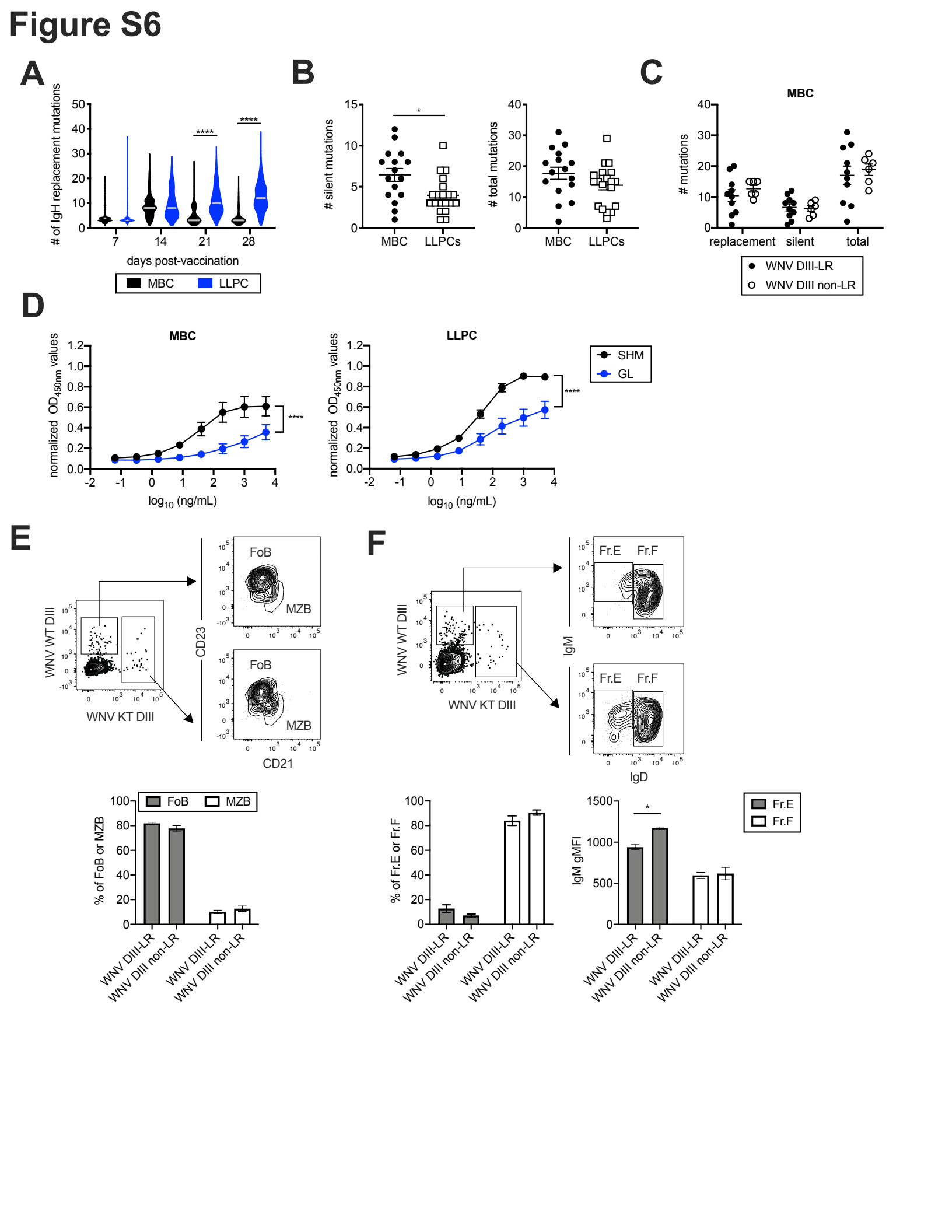
A
# of IgH replacement mutations
days post-vaccination
MBC
LLPC
B
silent mutations
total mutations
MBC
LLPCs
C
MBC
mutations
replacement
silent
total
WNV DIII-LR
WNV DIII non-LR
D
MBC
LLPC
normalized OD450nm values
log10 (ng/mL)
SHM
GL
E
WNV WT DIII
WNV KT DIII
CD23
CD21
FoB
MZB
% of FoB or MZB
F
Fr.E
Fr.F
IgM
IgD
% of Fr.E or Fr.F
IgM gMFI

Figure S6, related to Figure 6. WNV DIII-LR and WNV DIII non-LR naïve and precursor cells are not selected from distinct B cell subsets.

(**A**) WT mice were immunized with inactivated WNV vaccine. WNV DIII^{+} MBCs ($CD19^{+}GL7^{-}IgD^{-}IgM^{-}CD80^{+}CCR6^{+}$) and WNV DIII+ bone marrow PCs ($CD138^{hi}IgM^{-}$) were sorted at different time points and IgG repertoire analysis was performed by MiSeq. The total number of replacement mutations for IgH is shown for each week. Mean ± SEM are shown. ****p < 0.0001; Kruskal-Wallis test. (**B**) The number of silent and total mutations in the heavy and light chains of the isolated panels of mAbs are plotted. Mean ± SEM are shown; each symbol represents one mAb. *p < 0.05; Mann-Whitney test. (**C**) The number of replacement, silent, and total mutations found in DIII-LR and DIII non-LR specific mAbs from the MBC compartment. (**D**) ELISA binding curves for WNV SVPs are compared for germline-reverted and somatically-mutated mAbs from MBCs and LLPCs. Mean ± SEM are shown. Mean ± SEM are shown. ****p < 0.0001; two-way ANOVA. (**E**) Spleens from naïve mice were enriched for WNV WT and KT DIII tetramers binding. Frequencies of antigen-specific cells in the follicular (FoB) and marginal zone (MZ) B cell compartments were enumerated by flow cytometry. A representative flow cytometry plot is shown on the left and quantified on the right. Mean values ± SEM are shown. (**F**) Frequencies of WNV DIII-LR and WNV DIII non-LR-specific cells in Hardy Fractions E (Fr. E) and F (Fr. F) were enumerated by flow cytometry. A representative plot is on the left and quantification is shown in the middle. The IgM geometric mean fluorescence intensities (gMFI) of WNV DIII-LR and WNV DIII-non LR specific cells in Hardy Fractions E and F are quantified on the right. Mean values ± SEM are shown. *p < 0.05; matched 2-way ANOVA.

Figure S7

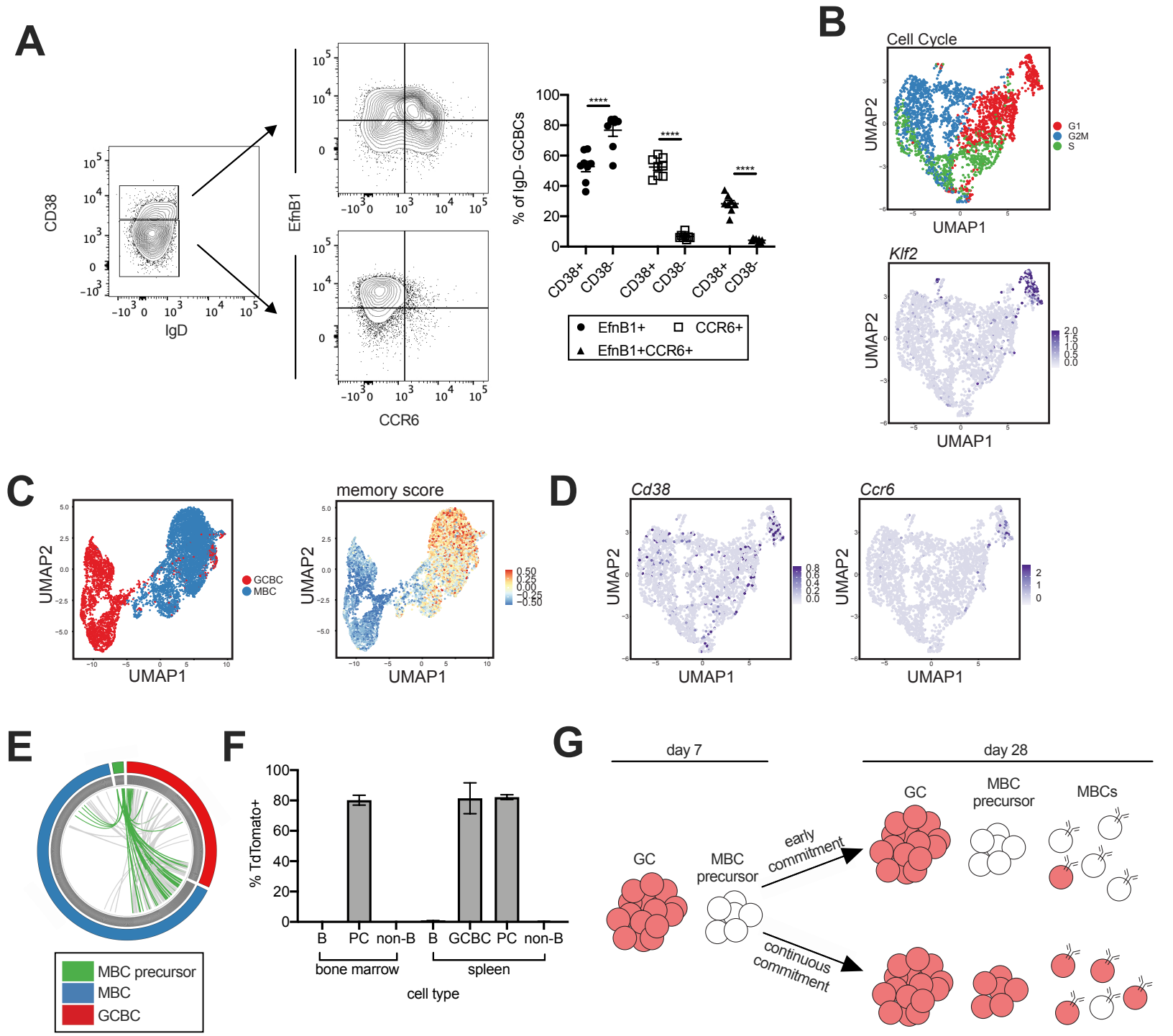
A
CD38
IgD
EfnB1
CCR6
% of IgD- GCBCs
CD38+
CD38-
EfnB1+
CCR6+
EfnB1+CCR6+
B
Cell Cycle
UMAP1
UMAP2
G1
G2M
S
Klf2
C
GCBC
MBC
memory score
D
Cd38
Ccr6
E
MBC precursor
MBC
GCBC
F
% TdTomato+
B
PC
non-B
GCBC
bone marrow
spleen
cell type
G
day 7
day 28
GC
MBC precursor
early commitment
continuous commitment
MBCs

Figure S7, related to Figure 7. Single cell RNA sequencing and lineage tracing validation.

(**A**) MBC precursor cells in polyclonal GC B cells ($CD19^+GL7^+IgD^-$) were identified using CD38, EfnB1, and CCR6 as markers. Example gating strategy to identify the MBC precursors is shown on the left and frequencies were quantified on the right. Mean ± SEM are shown. Data are from one experiment where each symbol represents one mouse. ****$p < 0.0001$; two-way ANOVA. (**B**) UMAP plots indicating cell cycle stage for each cluster (top) and *Klf2* gene expression (bottom). (**C**) Polyclonal swIg $CD80^+CCR6^+$ MBCs were sorted from wild-type mice vaccinated with WNV one week prior. scRNA profiles of mature GC B cells (as in **Figure 7A**) with the sorted MBCs (left) and computed MBC module score (right). (**D**) UMAP plot displaying *Cd38* and *Ccr6* gene expression levels in individual cells. (**E**) Clonal overlap between DIII-specific MBC precursors, DIII-specific GC B cells, and polyclonal MBCs are displayed as links between all three populations. (**F**) Jchain expression in GC B cells was confirmed by crossing Jchain to LSL-TdTomato mice and administering tamoxifen for two weeks. TdTomato expression was quantified for B cells ($CD19^+$ in the spleen or $B220^+$ in the bone marrow), plasma cells (PC, $CD138^+$), non-B cells ($B220^-CD138^-$ in bone marrow, $CD19^-GL7^-CD138^-$ in spleen), and GC B cells ($CD19^+GL7^+$). Mean values ± SEM are shown. (**G**) Expected results for TdT-Jchain mice if MBCs are committed early and continue to participate in GCs or if there is continuous selection of MBCs.

Primer name	Primer sequence
Aicda_237918_F	AGCCCCTCAGCCCTTTAATC
Aicda_237918_R	AGCTGGTGTTGTGTGCGAAG
CAS_R1_Term	TCGTGGTATCGTTATGCGCC
Jchain WT_F	TGCTGTGCAGATGATTAGG
Jchain Tg_F	CCCACATCAGGCACATGAGTAACAA
Jchain common_R:	CTCCTTGAGCAGACATGAGGATT

Table S3. Primers used to genotype transgenic mice, related to STAR Methods.